Electronic structure of α_t-(BEDT-TTF)$_2$I$_3$: A photoemission study

S. Söderholm and P. R. Varekamp
Materials Physics, Department of Physics, Royal Institute of Technology, S-100 44 Stockholm, Sweden

D. Schweitzer
3. Physikalisches Institut, Universität Stuttgart, Pfaffenwaldring 57, D-70550 Stuttgart, Germany
(Received 9 November 1994; revised manuscript received 18 May 1995)

Photoemission experiments have been performed on *in situ* cleaved crystals of the organic superconductor α_t-(BEDT-TTF)$_2$I$_3$. Nine distinct features are observed in the valence-band regime with binding energies between 1.4 and 11.2 eV. None of the valence-band structures shows dispersion along the Γ-Z (k_z) direction, i.e., perpendicular to the conducting BEDT-TTF layers. The spectral intensity is zero at, and to within about 0.5 eV below the Fermi level. This is ascribed to the presence of a fairly large band gap in this direction, in agreement with band-structure calculations. The photoemission spectrum of the valence band shows remarkable changes when the photon energy is changed. These changes are qualitatively understood as a cross-section dependence. The observed photon energy dependence suggests that both p orbitals and the lower-lying s orbitals of the atoms constituting the BEDT-TTF molecule contribute significantly to the molecular orbitals forming the valence band. Core-level spectroscopy on the I 4d and S 2p levels revealed no surface or chemically shifted components. The large width of these core levels is ascribed primarily to phonon broadening, although a contribution from disorder cannot be completely ruled out.

I. INTRODUCTION

Organic conductors with the composition (BEDT-TTF)$_2$I$_3$, where BEDT-TTF is an abbreviation for bis(ethylenedithio)-tetrathiafulvalene, exist in several crystallographic phases; see, for instance Refs. 1 and 2. The different phases have similar structures; they consist of alternating sheets of BEDT-TTF and I_3^-. In spite of this, the different phases have very different physical properties, e.g., the α phase undergoes a metal-to-insulator transition at 135 K,[3] but the β phase has a superconducting ground state, $T_c \approx 1.5$ K.[4] Although these molecular solids have been extensively studied, the information on their electronic structure is sparse, and the mechanism behind the superconductivity and type of superconductivity are still open questions. A powerful tool in studies of the electronic structure of solids is photoelectron spectroscopy, but such investigations on conducting molecular solids, i.e., charge-transfer (CT) complexes, have been hampered by difficulties in obtaining surfaces clean enough to utilize this technique. Photoelectron-spectroscopy studies on this class of materials have so far been on *in situ* prepared thin films of a few systems, i.e., TTF-TCNQ and other TCNQ compounds,[5,6] (DCNQI)$_2X$ [7] and α-(BEDT-TTF)$_2$I$_3$,[8,9] with one exception, (DCNQI)$_2$Cu, where the experiments were performed on crystals.[10,11] The samples were either grown and transferred under an inert atmosphere to the analysis chamber[10] or *in situ* mechanically cleaned crystals.[11] (For photoelectron spectroscopy on other classes of organic conductors, such as polymers, see, for instance, Ref. 12 and references therein.) In this paper angular-resolved normal emission photoemission spectra of the valence-band regime, the S 2p and the I 4d core level of α_t-(BEDT-TTF)$_2$I$_3$ crystals cleaved *in situ* are presented. Among the different phases of (BEDT-TTF)$_2$I$_3$ the α_t-phase was studied for technical reasons and because of physical considerations. The α_t phase is obtained by heating the α phase for some hours or days, depending on the temperature.[13,14] The α_t crystals are c-axis oriented and have a mosaic structure in the a-b plane due to internal stress during the transformation. The mosaicity of the α_t crystals has so far prevented a complete structural determination of this phase, but the unit-cell data and the molecular arrangement are the same as for the β phase.[15] [The unit cell is described by $a=6.615$ Å, $b=9.097$ Å, $c=15.291$ Å, $\alpha=94.35°$, $\beta=95.55°$, and $\gamma=109.75°$ (Refs. 3 and 15).] The similarity between the α_t and the β phase is also evident from spectroscopic data, e.g., Raman, ir, and NMR.[13–18]

II. EXPERIMENT

The photoemission experiments were performed at the toroidal grating monochromator beamline at the MAX Synchrotron Radiation Laboratory in Lund, Sweden. The spectra were recorded with a goniometer-mounted modified VSW hemispherical angle-resolving electron energy analyzer, acceptance $\pm 1°$. For a comprehensive description of the beamline, see Karlsson *et al.*[19] A thoroughly sputtered Ta foil in electrical contact with the sample was used as a reference for the Fermi level, and from the width of the tantalum Fermi edge the total-energy resolution of the spectra, photon, and electron contributions, was determined. For the valence-band spectra the resolution was determined to be 0.25 eV at a photon energy of 21 eV, 0.35 eV at $h\nu=100$ eV, and 0.55

eV at $h\nu = 150$ eV. The presented core-level spectra were recorded with a higher resolution: $\Delta E = 0.5$ eV for the S $2p$ spectra and 0.28 eV for the I $4d$ spectra.

The small size of the samples made it necessary to modify the standard sample holder system in order to reduce the influence of the background as much as possible. The sample holder is a Mo disc, $\phi = 20$ mm, with a bayonet joint so samples can be transferred between a load-lock chamber, a preparation chamber, and the analysis chamber. On this disc a cylindrical post was attached, which had a length of 5–6 mm and a cross section such that the sample covered most or all of it. The sample was glued to the post with a conducting ultrahigh-vacuum-compatible epoxy, and on the other side of the crystal another post was glued. During the curing of the epoxy, ~6 h at ~90–100 °C, the phase transition from α to α_t took place. By applying a force to the outer post, the crystal was cleaved perpendicular to the c axis. The samples used in the present study had areas of $\sim 3\times 2$ and $\sim 2\times 1$ mm^2. The surface of the crystals was smooth and had a black-brownish color. The crystals appear blacker if they are thicker. The surface of a cleaved crystal is not as shiny as the surface of electrochemically grown α and β crystals but rather looks more like an unpolished metal surface. In other words the surface of the cleave appears similar to the surface of c-axis-oriented thin films of the nonsuperconducting α phase, hereafter denoted α_f. This could be because of the mosaic structure of α_t crystals and/or the thickness of the samples. As the unit-cell parameters and the molecular arrangement are the same as for the α_t and β phases, it is evident from the crystal structure that the cleavage will occur between the weakly bonded BEDT-TTF and I_3^- layers.

The samples were carefully aligned, and several test spectra were recorded to ensure that the influence of the background (epoxy and sample holder) was negligible. In order to excite both orbitals in the plane of the surface and perpendicular to it, the photon angle of incidence was 45°. No changes in the recorded spectra of α_t were detected during the measurements. The based pressure in the analysis chamber, where the crystals were cleaved, was $< 2.5\times 10^{-10}$ mbar.

III. RESULTS AND DISCUSSION

Figure 1 shows photoemission spectra of an α_t crystal obtained in normal emission with different photon energies in the range 21–150 eV. The spectra in this figure are normalized to equal height in order to facilitate a comparison of how the relative intensity of the different structures varies with the photon energy, and to make as many of the structures in the different spectra as visible as possible. The presence of I $4d$ peaks because of second-order light made it impossible to record meaningful spectra with photon energies between about 45 and 55 eV. Such intensity is seen in the 54-eV spectrum above the Fermi level. Higher-order light also gives rise to a small hump at E_F in the 25-eV spectrum.

Nine distinct structures (labeled A to I in Fig. 1) can be observed in the valence-band regime, though not all structures can be observed in every spectrum. These structures have binding energies (E_b) between 1.4 and 11.2 eV relative to the Fermi level $E_F = 0$. Each structure is illustrated with a tick mark in the figure, which indicates the binding energy of the structure. Those structures that could be determined with certainty are indicated by a solid tick mark, while weaker structures are depicted by a dashed tick mark.

Figure 1 shows that the structures A, B, C, D, E, H, and I, when they are visible, have binding energies that are independent of the exciting photon energy. The deviations of the binding energies of each structure from a constant value are random and at the most 0.10–0.15 eV for a particular structure, i.e., well within the experimental resolution. The binding energies of structures F and G show larger changes, however, up to 0.3 eV, and the changes of binding energy with photon energy do not seem to be random.

Note that the shape changes of the spectra in the (2.5–4.5)-eV binding-energy range, taken as a whole, strongly support the presence of two separate structures

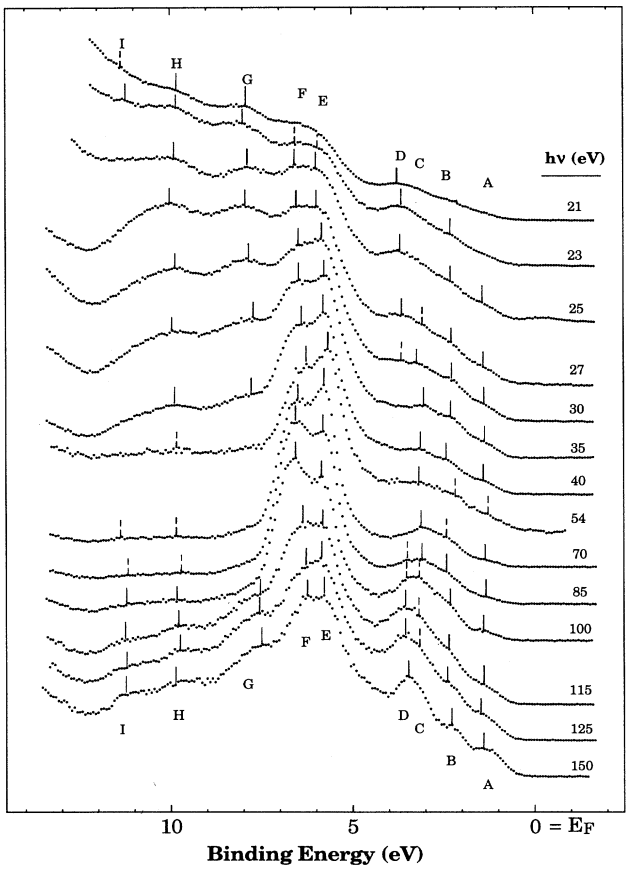

FIG. 1. Valence-band photoemission spectra of α_t-(BEDT-TTF)$_2$I$_3$ obtained in normal emission with photon energies between 21 and 150 eV. Different structures in the valence-band regime are labeled A–I and marked with tick marks in the spectra. (Weak features are indicated by a dashed tick mark.)

C and D, although this is not obvious when the spectra are viewed individually. A probable explanation for the nonrandom changes in the binding energies of structures F and G with photon energy is that these structures are composed of two or more unresolved structures. The variations of the intensities of these closely lying peaks with photon energy then result in an apparent shift of the whole unresolved structure. The shape changes of structure F give evidence for this explanation. The fact that structure G appears at two different binding energies, one at high photon energies and another at low photon energies also supports this explanation. (A careful inspection shows that structure D also tends to appear at two different binding energies as well, but the difference is small, <0.12 eV.) Further support for the presence of several unresolved structures within structures F and G is given by the comparison of the α_t spectra with the gas-phase spectrum of BEDT-TTF; see below.

Thus, the present investigation gives no support for dispersing bands in the Γ-Z (k_z) direction. The lack of dispersion in this direction is in agreement with the two-dimensional electronic structure of the BEDT-TTF salts deduced from galvanometric and optical measurements.[1]

The valence-band regime spectra also show that there is no spectral intensity at the Fermi level along the Γ-Z line in the Brillouin zone; a finite intensity is only seen for binding energies larger than about 0.5 eV. At the highest photon energies a finite intensity exists about 0.4 eV below E_F and at the lowest roughly 0.7 eV below. The reason for this is that a larger part of the Brillouin zone is probed when the photon energy is increased, since the angular resolution is constant, i.e., $\Delta k_{\parallel} \propto \sqrt{E_k}$, where E_k is the kinetic energy of the emitted photoelectrons.

The photon energy dependence of the spectral intensity of the different structures in the valence-band regime gives rise to remarkable changes of the spectrum when the photon energy is changed (see Fig. 1). The most striking change when the photon energy is increased, from 21 eV, is the growth of the relative intensity of peaks E and F. Their relative intensities increase when the photon energy is increased and then go through a broad maximum before starting to decrease at the highest photon energies. The broad maximum occurs between photon energies of 40 and 110 eV and has its maximum at about 80 eV.

In order to get some information about the mechanism behind the intensity variations, the intensity of each structure was calculated as a function of the excitation photon energy. As a first step in the calculation of the intensities, the spectra were normalized with respect to the photon flux, and an exponential background was subtracted. Attempts to fit these spectra by a least-squares fit, with the appropriate number of peaks, failed because of the large number of parameters if the peaks were allowed to have different full widths at half maximum (FWHM's). Thus, it was assumed that all peaks were pure Gaussians with the same FWHM. The intensity of each feature in the valence band was then determined from the height of the different peaks. The maximum error, due to using the same full width at half maximum, is estimated to about 25%. This error is negligible in comparison with the intensity differences between the different components and the changes of intensity of a particular structure with photon energy; see Fig. 2. This figure shows that the photon energy dependences of the absolute intensity of all valence-band structures are actually quite similar. The behavior of E and F is slightly different at the highest photon energies. Overall, the intensity of each feature oscillates around a slowly decreasing background when the photon energy is increased; see Fig. 2. Local maxima appear for photon energies of about 30, 80, and 120 eV. Structures E and F do not have a maximum at $h\nu \approx 120$ eV; instead the intensity of these structures decreases monotonically for $h\nu > 85$ eV.

Attempts to fit the extrema in the intensity to critical points in the Brillouin zone failed. These fits gave extrema not coinciding with the experimentally determined ones, except for the two extremas used as input in the fit and/or unreasonable values for the inner potential.

However, the photon energy dependence of the spectral intensity can be qualitatively understood as a cross-section dependence. In Fig. 2 the calculated atomic cross sections for C 2s, C 2p, S 3s, and S 3p are shown.[20] There exists a consensus that the valence band in organic conductors is formed by molecular orbitals derived mainly from the highest-lying atomic orbitals of the atoms forming the molecule. In the present case, these orbitals are the C 2p and S 3p orbitals. Their cross sections indicate that the maximum around $h\nu = 80$ eV is due to the local

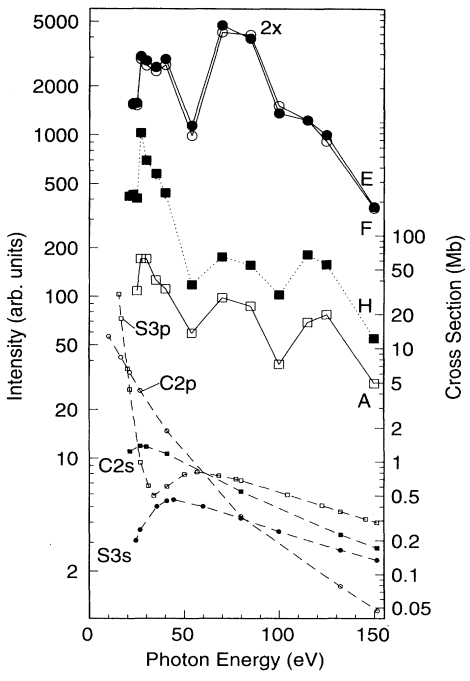

FIG. 2. The spectral intensity of structures A, E, F, and H, in the valence band, and the calculated atomic cross section for C 2s, C 2p, S 3s, and S 3p (Ref. 20) as a function of the photon energy. The lines are guides to the eye. The intensities of E and F are scaled by a factor of 2 for clarity.

maximum in the S 3p cross section in this photon energy regime. The fact that structures E an F are more enhanced in this regime implies that the S 3p contribution is larger in the molecular orbitals giving rise to these bands than in the other bands forming the valence-band regime. The increase in intensity for $h\nu < 54$ eV reflects the rapidly and monotonically increasing cross section of C 2p and S 3p in this regime. The appearance of a shoulder on the intensity curves for photon energies around 40 eV can in this picture be ascribed to a local maximum in the S 3s cross section. The more pronounced shoulder seen in the curves corresponding to E and F reflects the larger contribution from S to these bands; cf. the discussion above. The decrease in the intensity seen for $25 < h\nu < 27$ can also be ascribed to a cross-section effect due to s-orbital contributions to the electronic structure of the valence band. The sudden decrease in the spectral intensity suggests that this minima is not related to local maxima in the C 2s and S 3s cross sections. Assuming that the molecular orbitals forming the valence band can be viewed as linear combinations of atomic orbitals, this sudden decrease in intensity occurs because of the photon energy being too small to excite contributions from C 2s and/or S 3s. The observed photon energy dependence suggests that it is not sufficient to discuss the electronic structure of organic conductors only in terms of the highest-lying atomic orbitals of the atoms forming the organic molecule, since even molecular orbitals forming bands close to the Fermi level has a non-negligible contribution from deeper-lying orbitals. In the present case, s orbitals contribute to structures A and B, since they show a similar behavior. The intensity variations of structures C and D, in the photon energy regimes where they are visible, suggests that these structures also have a similar photon energy dependence. A linear combination of the calculated cross sections from carbon, sulphur, and iodine cannot, however, explain the intensity maximum near 120 eV.

Additional information about the origin of the valence-band features can be obtained by comparing the photoemission spectrum of α_t with the spectrum of α_f and gas-phase spectra of BEDT-TTF. Since α_t has a superconducting ground state with $T_c = 8$ K (Refs. 13 and 14) and is c-axis ordered, c^* photoemission data from this phase is suitable for comparison with c^* data from α_f, i.e., c-axis-oriented thin films of the nonsuperconducting α phase, which has been studied previously.[8,9] (The spectrum of α_f is compared with gas-phase of BEDT-TTF and other related donors in Ref. 8.) Such a comparison can be done, since for many organic compounds the photoemission spectra of the gas phase and the solid are similar. The main difference is the bands in the spectrum of the solid being broadened and rigidly shifted in comparison with the gas-phase spectrum.[21–23] Even in the case of charge-transfer complexes, features in the valence band can be traced back to bands in the gas-phase spectra[5,8] and/or in the spectrum of the neutral donor (or acceptor).[24] This implies that the electronic structure of the complex is primarily governed by the electronic structure of the different molecules forming the solid, at least when the solid consists of distinct molecular species.

Figure 3 in this paper shows a comparison between schematic representations of the gas-phase spectrum of BEDT-TTF,[25] the spectra of α_f,[8] α_t, and the binding energy of the calculated energy bands of β-(BEDT-TTF)$_2$I$_3$ at Γ.[26] In this figure the proposed alignment of the BEDT-TTF and the α_f spectrum is used, and the α_t spectrum has been aligned by placing $E_b = 0$ in the same position as $E_b = 0$ for the α_f spectrum. (An alignment of the α_t spectrum so that the best coincidence with the gas-phase spectra is obtained corresponds to a small shift,

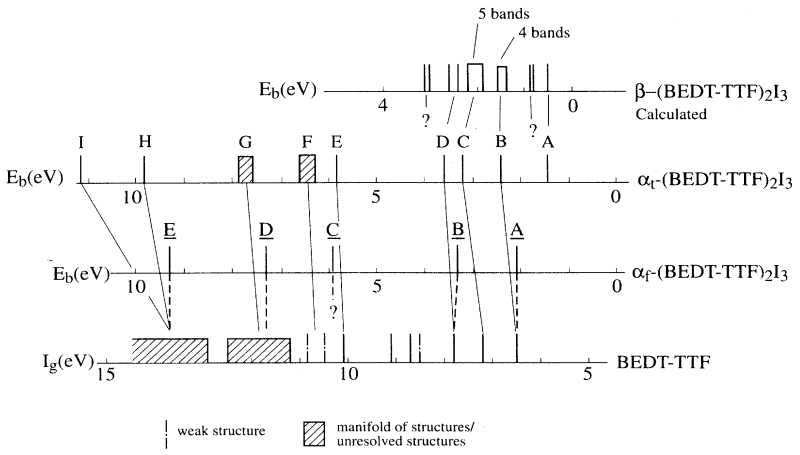

FIG. 3. Schematic representation of the photoemission spectrum of (from the bottom up) a BEDT-TTF gas phase (Ref. 25), an α-(BEDT-TTF)$_2$I$_3$ film (Ref. 8), an α_t-(BEDT-TTF)$_2$I$_3$ crystal, and the binding energy of the calculated energy bands of β-(BEDT-TTF)$_2$I$_3$ at Γ (Ref. 26). The bars represent structures in the different spectra; weak ones are indicated by broken bars, and the hatched areas represent manifolds of structures or unresolved/poorly resolves structures. Tentative correspondence between features in different spectra are indicated by thin lines and by broken lines. The energy scale of the gas phase spectra is the ionization potential with respect to the vacuum level.

about 0.20 eV, towards lower binding energy.) The calculated bands are aligned so the position of structure A in α_t coincides with the band closest to the Fermi level. The five distinct features in the valence-band regime of α_f are labeled $\underline{A}-\underline{E}$ in Fig. 3 and in the following discussion. The alignment between α_f and α_t given in the figure indicates that $\underline{B}$ and $\underline{C}$ are split into two structures each, C and D, and E and F, respectively. Thus α_t gives a better agreement with the gas-phase spectrum of BEDT-TTF than α_f. This comparison also suggests that the apparent shift of binding energy with the photon energy of F occurs because of the presence of (two) unresolved structures corresponding to two weak structures in the gas-phase spectrum of BEDT-TTF. G and H, which correspond to $\underline{D}$ and $\underline{E}$, each arise from a manifold of structures in the gas-phase spectrum of BEDT-TTF. These structures are shifted to higher binding energies by about 0.5 eV with respect to the corresponding structures in the α_f and BEDT-TTF spectrum. Similar to the explanation for structure F, the comparison with the gas-phase spectrum of BEDT-TTF suggests that structure G could be due to several unresolved structures causing the binding energy to shift with the photon energy. The fact that more structures are seen in the valence band of α_t than in the valence band of α_f could reflect differences in the electronic structure of the compounds, but another cause could be disorder, which could broaden structures. Although both compounds are disordered, the disorder is less in the α_t samples. It is also interesting to note that neither the spectrum of α_t nor the spectrum of α_f show any traces of the molecular orbitals with ionization potentials of about 9 eV; as discussed in Ref. 8 other alignments of the spectra also cause molecular orbitals with $I_g=9-10$ eV to lack corresponding levels in the α_f and α_t spectra.

The proposed tentative correspondence between the different spectra implies that structure A in the photoemission spectrum of α_t cannot be readily said to arise from the lowest-lying π orbitals of the BEDT-TTF molecule. There are several plausible reasons for this; for instance, structure A can be due to the partially filled band, which causes the compound to show metallic properties. In this case the presence of holes in the band formed by the highest occupied molecular orbital of BEDT-TTF could change the electronic structure of α_t in the vicinity of E_F considerably in comparison to the electronic structure of the neutral donor but only have a minor influence on the deeper-lying bands.

Another cause for the absence of any correlation between A and BEDT-TTF could be the donor-anion interaction, which takes place via C-H $\cdots$ I contacts, i.e., perpendicular to the conducting BEDT-TTF layers. Recently Moldenhauer *et al.* have shown that this interaction affects the CH_2 stretching frequency in different phases of (BEDT-TTF)$_2$I$_3$ and other BEDT-TTF complexes,[27] which have different critical temperatures. This finding suggests that the electronic structure close to E_F, where A is located, is affected by the electronic donor-anion interaction, i.e., a three-dimensional interaction causes the electronic structure of the CT complex to be different from the structure of the neutral donor (acceptor). Changes in T_c due to changes in the phonon spectrum are probably small, since the stretching frequency is about 2900 cm^{-1}.

Although there exists no band-structure calculation for α_t, since the crystal structure is not known, a comparison with calculations for the β phase is justified by their similar crystal structures[15] and spectroscopic properties[13-18] and by the fact that the calculated band structure for β-(BEDT-TTF)$_2X$ ($X^-=I_3^-$, AuI_2^-, IBr_2^-) within the same method are similar.[26,28] Figure 4 shows the result of the only calculation for the β phase that considered more than the two highest occupied bands.[26] This self-consistent-field calculation using the pseudofunction method is also the only one predicting a dispersion (less than 50 meV) in the Γ-Z direction for some of the bands. The best correspondence between the calculated band structure and the experimental data is obtained if structure A is aligned with the band closest to the Fermi level. As seen from Fig. 3, the correspondence between α_t and the calculation is fair. However, the electronic structure in the k_x-k_y plane must be experimentally determined for β-(BEDT-TTF)$_2X$ before any firm conclusions can be drawn about the ability of the employed method to pre-

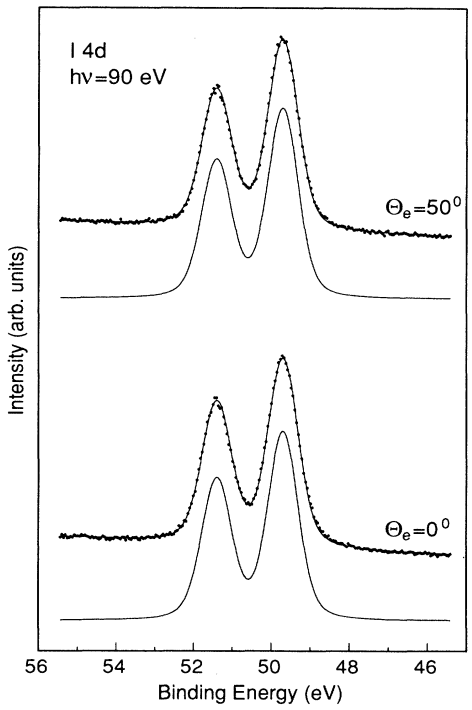

FIG. 4. I 4*d* core-level spectra, excited with a photon energy of 90 eV. The points represent the experimental data, recorded at different emission angles; bottom 0° and top 50°. The full lines are the result of a curve fitting procedure. The parameters used are given in the text.

dict the band structure of organic conductors.

Band structures calculated for β-(BEDT-TTF)$_2$I$_3$ with different methods[26,28,29] all predict a band gap in the Γ-Z direction, with the valence-band maximum situated 0.5–0.7 eV below the Fermi level; however, the predicted dispersions in the Γ-Z and other directions depend on the method. Thus, the measured value for the valence-band maximum of α_t obtained with the smallest Δk, 0.7 eV, is in good agreement with the calculations. The lack of a finite spectral intensity at the Fermi level, although α_t shows metallic galvanometric properties, must be due to a fairly large band gap in the Γ-Z direction. The absence of a Fermi edge due to indirect transitions can, in the present case, be ascribed to the low electron density in α_t, which is a factor 10–100 smaller than in ordinary metals, and also to a low probability for photoelectron excitations in α_t. Other possible explanations can be ruled out. For example, a Luttinger liquid would lack spectral intensity at E_F, but α_t has a two-dimensional electronic structure, and, to our knowledge, it has not been proved that a two-dimensional Luttinger liquid exists. An alternative explanation for the lack of a Fermi edge depends on the entire surface consisting of neutral BEDT-TTF molecules. Although the presence of neutral BEDT-TTF molecules have been observed previously on the surface and/or in the near surface region of α_t,[14,15,18] neutral BEDT-TTF molecules cannot completely cover the surface in the present case, as the samples were cleaved after the heat treatment, and thus the studied surface corresponds to the interior of the heat-treated crystal. Furthermore, there is no indication in any of the recorded valence-band or core-level spectra of neutral BEDT-TTF in the near surface region.

In scans over an extended binding-energy range, two shallow core levels (inner valence states) were observed at $E_b = 14.2$ and 18.3 eV. The former is giving rise to the upturn of the spectra in Fig. 1 at the highest binding energies. These structures are broad, with widths of about 2 eV and 7 eV, respectively. The intensity of the latter decreases with decreasing photon energy, while the intensity of the other structure is roughly independent of the photon energy. Although these structures cannot be unambiguously assigned to certain levels, the two candidates are C 2s and S 3s. Furthermore, it is not clear to which extent the two observed levels mix with the valence band or if they are a part of it. I 5s can be ruled out as an origin, since in the study of α_f two shallow core levels at similar energies were also observed even in iodine-deficient films.[8] Since a structure with $E_b \approx 13-14$ eV is seen in the spectra of other organic conductors with and without sulphur, e.g., Pt-phthalocyanine radical salts,[24] poly-3-hexylthiophene/NOPF$_6$,[30] polypyrrole,[31] and polyacetylene,[32] this structure is most likely associated with C 2s σ-type orbitals. The present data do not allow an unambiguous assignment of the other shallow core level; it could either originate from S 3s or C 2s orbitals or originate from many-body effects.[32]

The I 4d core level was recorded at two different emission angles, 0° and 50°, as shown in Fig. 4. From a fitting procedure the binding energy for the $4d_{5/2}$ level was determined to be 49.7 eV and the spin-orbit splitting to be 1.71 eV. The simulated line shape was obtained through a convolution of a Lorentzian and a Gaussian function. The latter simulates broadening of the spectrum due to the resolution of the apparatus, phonons, and disorder. The former represents the limited lifetime of the core hole created by the excitation. The FWHM for the Lorentzian line was 0.26 eV and was 0.77 eV for the Gaussian line. (Rather good fits could be obtained with Lorentzian linewidths down to 0.22 eV if the Gaussian linewidth was increased; e.g., for a Lorentzian FWHM of 0.22 eV the Gaussian FWHM was 0.80 eV.) When the emission angle was changed from 0° and 50° the branching ratio had to be changed from 1.333 to 1.380 in order to fit the experimental data. This small change can be ascribed to changes in the background and/or diffraction effects. The fact that the spectra can be fitted well with one component and that the only difference between spectra recorded at different emission angles is a small change of the branching ratio implies that all iodine is present as I_3^-, and that no I_3^- is situated close to or at the surface, the a-b plane. This is in agreement with scanning tunneling microscopy on α (Ref. 33) and β-(BEDT-TTF)$_2$I$_3$ (Ref. 34), which revealed no iodine on the surface of the crystals. This has been attributed to

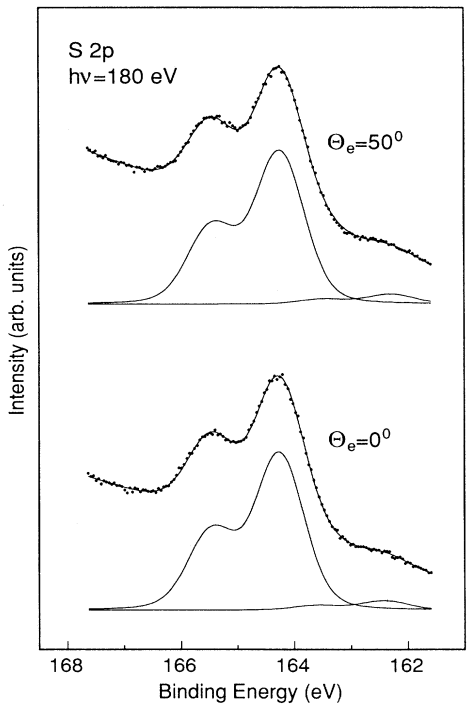

FIG. 5. S 2p core-level spectra, excited with a photon energy of 180 eV. The points represent the experimental data, recorded at different emission angles; bottom 0° and top 50°. The full lines are the result of a curve fitting procedure. The parameters used are given in the text.

the instability of the anion layers.[34]

The instrumental resolution cannot explain the rather broad FWHM of the I 4*d* core level, since spectra recorded with a lower resolution ($\Delta E = 0.35$ eV) had the same FWHM and were fitted equally well with the same parameters. Thus, the rather broad Gaussian line needed to simulate the spectra is caused by phonon broadening and disorder. A large phonon-induced linewidth is consistent with organic conductors being "soft materials" in the sense that many phonons are excited at room temperature, and the large number of atoms in the unit cell makes many phonon modes possible. X-ray-diffraction experiments show that the thermal motion of the atoms in organic compounds causes the root-mean-square value of the displacement to be up to 0.5 Å. In inorganic compounds it is typically 0.05–0.10 Å.[35] Thus, it is proposed that phonon broadening dominates the linewidth; however, contributions from disorder cannot be ruled out. A low-temperature experiment could give information about the magnitude of the different contributions.

The S 2*p* spectrum is reproduced well by fitting the main doublet with one spin-orbit split component and, rather arbitrarily, fitting the weak structure seen around $E_b = 162$ eV with a doublet using the same parameters as for the main peak, i.e., a spin-orbit splitting of 1.2 eV, a branching ratio of 2, a Lorentzian FWHM of 0.2 eV, and a Gaussian FWHM of 0.9 eV (Fig. 5). From the fit the binding energy S $2p_{3/2}$ level was determined to be 164.3 eV. It should be noted that the spectra can be fitted equally well by using two components for the main peak if the Gaussian FWHM is set to 0.7 eV. These components have almost equal intensities, and the intensity ratio is nearly the same for the investigated emission angles.

Since the experimental data gives no clear support for more than one component, it is suggested that conceivable chemically shifted peaks and/or surface shifted peaks are not resolved mainly because of phonon broadening of the components. Furthermore, it is reasonable to assume that such a shift could be rather small in α_t, since the chemical environments of the different sulphur atoms in the BEDT-TTF molecule are similar, and the sulphur atoms closest to the surface are found some angstroms below it. For the same reasons as described above for the I 4*d* level, it is thus similarly likely that phonon broadening dominates the linewidth of S 2*p*. The increased Gaussian linewidth in comparison with the I 4*d* level, even if a more efficient screening of a core hole due to the metallic properties of the BEDT-TTF layer is considered, can be explained by a poorer instrumental resolution at a photon energy of 180 eV.

IV. SUMMARY

The electronic structure of the organic superconductor α_t-(BEDT-TTF)$_2$I$_3$ has been studied by photoelectron spectroscopy on *in situ* cleaved crystals. The valence-band regime consisted of nine distinct structures with binding energies between 1.4 and 11.2 eV, with respect to the Fermi level. Angular-resolved measurements showed no dispersion along the Γ-Z (k_z) direction, i.e., perpendicular to the conducting BEDT-TTF layers, for the structures in the valence-band regime. The spectral intensity was found to be zero down to about 0.5 eV below the Fermi level. This is ascribed to the presence of a band gap along Γ-Z, in agreement with band-structure calculations.

The shape of the valence-band spectrum showed remarkable changes when the photon energy was changed. The observed changes of the spectral intensity can be qualitatively understood as a cross-section dependence. The dependence of the spectral intensity on the photon energy suggests that contributions from C 2*s* and S 3*s* orbitals to the molecular orbitals forming the valence band are significant. This means that more than just the highest-lying orbitals, in the present case C 2*p* and S 3*p*, must be taken into account when the electronic structure of organic conductors is discussed.

The correspondence between structures in the valence-band spectrum of α_t-(BEDT-TTF)$_2$I$_3$ and the gas-phase spectrum of BEDT-TTF shows that the valence band originates from primarily molecular orbitals. This further increases the experimental foundation behind the idea that the electronic structure of a CT complex is governed by the electronic structure of the different molecules forming the solid. However, in contrast to *c*-axis-oriented thin films of α-(BEDT-TTF)$_2$I$_3$, the structure with the lowest binding energy in α_t cannot readily be said to arise from to the lowest-lying π orbitals of the BEDT-TTF molecule.

Two shallow core levels (inner valence states) with binding energies of 14.2 and 18.3 eV were observed. The origin of the former is most likely C 2*s* σ-type orbitals. The latter cannot be unambiguously assigned. The I 4*d* and the S 2*p* core levels were also studied. These measurements revealed no surface or chemically shifted components. The large width of these core levels is mainly, ascribed to phonon broadening in agreement with organic conductors being "soft materials," in the sense that many phonons are excited at room temperature and the large number of atoms in the unit cell makes many phonon modes possible, although some contribution from disorder cannot be ruled out.

[1]T. Ishiguro and K. Yamaji, *Organic Superconductors* (Springer, Berlin, 1990), Chap. 5.

[2]J. M. Williams, A. J. Schultz, U. Geiser, K. D. Carlson, A. M. Kini, H. H. Wang, W.-K. Kwok, M.-H. Whangbo, and J. E. Schirber, Science **252**, 1501 (1991).

[3]K. Bender, I. Hennig, D. Schweitzer, K. Dietz, H. Endres, and H. J. Keller, Mol Cryst. Liq. Cryst. **107**, 359 (1984); I. Hennig, K. Bender, D. Schweitzer, K. Dietz, H. Endres, H. J. Keller, A. Gleitz, and H. W. Helberg, *ibid.* **119**, 337 (1985).

[4]E. B. Yagubskii, I. F. Shchegolev, V. N. Laukhin, P. A. Kononovich, M. V. Kartsovnic, A. V. Zvarykina, and L. I. Bubarov, JETP Lett. **39**, 12 (1984).

[5]W. D. Grobman, R. A. Pollak, D. E. Eastman, E. T. Maas, Jr., and B. A. Scott, Phys. Rev. Lett. **32**, 534 (1974).

[6]P. Nielsen, A. J. Epstein, and D. J. Sandman, Solid State Commun. **15**, 53 (974); P. Nielsen, D. J. Sandman, and A. J. Epstein, *ibid.* **17**, 1067 (1975).

[7]D. Schmeisser, W. Jaegerman, Ch. Pettenkofer, H. Wachtel, A. Jimenez-Gonzales, J. U. von Schütz, H. C. Wolf, P. Erk, H. Meixner, and S. Hünig, Solid State Commun. **81**, 827 (1992); H. Wachtel, D. Schmeisser, J. U. von Schütz, and H. C. Wolf, Appl. Surf. Sci. **55**, 239 (1992).

[8]S. Söderholm, B. Loppinet, and D. Schweitzer, Synth. Met. **62**, 187 (1994).

[9]S. Söderholm, B. Loppinet, and D. Schweitzer, Synth. Met. **65**, 65 (1994).

[10]D. Schmeisser, K. Graf, W. Göpel, J. U. von Schütz, P. Erk, and S. Hünig, Chem. Phys. Lett. **148**, 423 (1988); D. Schmeisser, A. Gonzales, J. U. von Schütz, H. Wachtel, and H. C. Wolf, J. Phys. (France) I **1**, 1347 (1991).

[11]I. H. Inoue, A. Kakizaki, H. Namatame, A. Fujimori, A. Kobayashi, R. Kato, and H. Kobayashi, Phys. Rev. B **45**, 5828 (1992); I. H. Inoue, M. Watanabe, T. Kinoshita, A. Kakizaki, R. Kato, A. Kobayashi, H. Kobayashi, and A. Fujimori, *ibid.* **47**, 12 917 (1993).

[12]*Proceedings of the International Conference on Science and Technology of Synthetic Metals, Tübingen, 1990* [Synth. Met. **41-43**, (1991)], *Proceedings of the International Conference on Science and Technology of Synthetic Metals, Göteborg, 1992* [Synth. Met. **55-57** (1993)].

[13]G. O. Baram, L. I. Buravov, L. C. Degtariev, M. E. Kozlov, V. N. Laukhin, E. E. Luakhina, V. G. Orischenko, K. I. Pokhodnia, M. K. Scheinkman, R. P. Shibaeva, and E. B. Yagubskii, JETP Lett. **44**, 293 (1986).

[14]D. Schweitzer, P. Bele, H. Brunner, E. Gogu, U. Haeberlen, I. Hennig, I. Klutz, R. Świetlik, and H. J. Keller, Z. Phys. B **67**, 489 (1987).

[15]S. Kahlich, S. Gärtner, D. Schweitzer, and H. J. Keller, Synth. Met. **41-43**, 2019 (1991).

[16]I. Hennig, U. Haeberlen, I. Heinen, D. Schweitzer, and H. J. Keller, Physica C **153-155**, 493 (1988).

[17]S. Gärtner, D. Schweitzer, and H. J. Keller, Synth. Met. **41-43**, 2059 (1991).

[18]A. Graja, K. I. Pokhodnia, M. Weger, and D. Schweitzer, Synth. Met. **55-57**, 2477 (1993); R. Świetlik, D. Schweitzer, and H. J. Keller, Phys. Rev. B **36**, 6881 (1987).

[19]U. O. Karlsson, J. N. Andersen, K. Hansen, and R. Nyholm, Nucl. Instrum. Methods A **282**, 553 (1989).

[20]J. J. Yeh and I. Lindau, At. Data Nucl. Data Tables **32**, 1 (1985).

[21]W. D. Grobman and E. E. Koch, in *Photoemisison in Solids,* edited by L. Ley and M. Cardona (Springer, Berlin, 1979), Vol. 2, p. 261-298.

[22]P. Nielsen, Phys. Rev. B **10**, 1673 (1974).

[23]N. Sato, H. Inokuchi, and I. Shirotani, J. Chem. Phys. **60**, 327 (1980).

[24]S. Hino, K. Matsumoto, H. Yamakado, K. Yakushi, and H. Kuroda, Synth. Met. **32**, 301 (1989).

[25]N. Sato, G. Saito, and H. Inokuchi, Chem. Phys. **76**, 79 (1983).

[26]R. V. Kasowski and M.-H. Whangbo, Inorg. Chem. **29**, 360 (1990).

[27]J. Moldenhauer, Ch. Horn, K. I. Pokhodnia, D. Schweitzer, I. Heinen, and H. J. Keller, Synth. Met. **60**, 31 (1993).

[28]M.-H. Whangbo, J. M. Williams, P. C. W. Leung, M. A. Beno, T. J. Emge, H. W. Wang, K. D. Carlson, and G. W. Crabtree, J. Am. Chem. Soc. **107**, 5815 (1985).

[29]T. Mori, A. Kobayashi, Y. Sasaki, H. Kobayashi, G. Saito, and H. Inokuchi, Chem. Lett. **1984**, 627 (1984).

[30]R. Lazzaroni, M. Lögdlund, S. Stafström, W. R. Salaneck, and J. L. Brédas, J. Chem. Phys. **93**, 4433 (1990).

[31]P. Bätz, D. Schweisser, and W. Göpel, Phys. Rev B **43**, 9178 (1991).

[32]M. P. Keane, A. Naves de Brito, N. Correia, S. Svensson, L. Karlsson, B. Wannberg, U. Gelius, S. Lunell, W. R. Salaneck, M. Lögdlund, D. B. Swanson, and A. G. MacDiarmid, Phys. Rev. B **45**, 6390 (1992).

[33]Y. F. Miura, A. Kasai, T. Nakamura, H. Komizu, M. Matsumoto, and Y. Kawabata, Mol. Cryst. Liq. Cryst. **196**, 161 (1991).

[34]M. Yoshimura, H. Shigekawa, H. Yamochi, G. Saito, Y. Saito, and A. Kawazu, Phys. Rev. B **44**, 1970 (1991).

[35]B. K. Vainshtein, Mod. Crystallogr. I (Springer-Berlin, 1981), Chap. 4.